Soft Matter

COMMUNICATION

View Article Online
View Journal | View Issue



Cite this: *Soft Matter*, 2025, **21**, 4999

Received 13th November 2024,
Accepted 1st June 2025

DOI: 10.1039/d4sm01343c

rsc.li/soft-matter-journal

# Microrheology of gel-forming airway mucins isolated from porcine trachea†

Elizabeth M. Engle,‡[ab] Sydney Yang,‡[a] Allison Boboltz,[a] Sahana Kumar,[ab] Alexa Stern[a] and Gregg A. Duncan*[ab]

**Mucus produced in the lungs has important protective barrier functions that strongly depend on its biomolecular composition, biopolymer network architecture, and viscoelastic properties. However, to date, there has yet to be a readily available source of reconstituted, gel-forming mucins from the lungs to model and study its biophysical properties. To address this, we established an in-house procedure to extract airway mucins from pig trachea with minimal DNA contamination consisting of ~70% by weight protein. Particle tracking microrheology was used to evaluate the biophysical properties of porcine trachea mucins for comparison to other reconstituted mucin and native mucus gels. At an ionic strength and pH reflective of conditions in the lungs, we found that porcine tracheal mucins formed a tighter mesh network and possessed a significantly greater microviscosity compared to mucins extracted from the porcine small intestine. In comparison to mucus harvested from human airway tissue cultures, we found that porcine tracheal mucins also possessed a greater microviscosity, suggesting that these mucins can form into a gel at physiological total solid concentrations.**

Mucus lines the epithelium of mammalian organs including the stomach, eyes, respiratory tract, and reproductive tract.[1] The mucus gel lining these tissues serves as a barrier against foreign particulates as well as providing lubrication and hydration.[2–4] Together, mucins secreted at epithelial surfaces function to form the mucus gel network through electrostatic interactions, entanglement, and polymerization *via* disulfide bonding within cysteine rich domains of mucin glycoprotein.[2,5,6] Mucus gels produced in distinct tissues possess unique biomolecular and biophysical properties depending on their precise functions. For example in the gut, a mucus gel layer exists with a loosely crosslinked, microbe-rich mucus layer overlying a more densely crosslinked, microbe-free mucus layer to physically separate the epithelium from the microbiome and other potentially pathogenic microbes.[7,8] Prior studies have shown that airway mucins can self-organize into strands and sheets to support mucociliary transport on the airway epithelial surface.[9,10] In addition, each mucin varies in its *O*-linked glycosylation pattern, which contains different functional groups such as terminal sulfate, sialic acid, and fucose groups.[6,11] Prior work has established that these terminal functional groups directly impact the ability of airway mucins to neutralize viral pathogens and prevent infection.[12–14] Thus, the structure and function of mucins is highly tailored to the tissue from which they arise.

Historically, mucins have been extracted from animal tissues, such as bovine submaxillary mucins (BSM), porcine small intestinal mucins (PSIM), and porcine gastric mucins (PGM).[15] These animal-derived mucins are unique in their physicochemical properties owing to the distinct gel-forming mucin types present in each mucosal tissue compartment. For example, mucins are produced regionally in the gastrointestinal tract with different compositions where mucin 5AC is produced in the stomach and mucin 2 is produced in the small intestine.[7] While PGM is available in bulk from commercial sources making it convenient for use, a previous report has shown that commercial PGM contains significant amounts of DNA as well as other contaminants and may be partially degraded due to its processing.[16] It is also important to note that mucins in the airway possess a unique composition, predominantly composed of mucin 5B and mucin 5AC,[2,5] that is distinct from other mucosal tissues. As a result, previously reported lab-extracted and commercial mucins do not provide models that are wholly representative of airway mucus. Airway derived mucins have been primarily sourced from human patient samples (*e.g.* sputum produced by cough,[17] mucus collected from endotracheal tubes (ETT)[18–20]) or from human airway tissue cultures grown at the air–liquid interface (ALI).[21–23] Unlike reconstituted lab-extracted mucins, mucus derived from *in vitro* human airway tissue cultures at ALI or *ex vivo* human patients may possess additional proteases, DNA, salts, and potentially other non-mucin proteins derived from cellular debris.[19] However, there are limitations in broader usage of

[a] *Fischell Department of Bioengineering, University of Maryland, College Park, Maryland, USA. E-mail: gaduncan@umd.edu*
[b] *Molecular and Cellular Biology Program, University of Maryland, College Park, Maryland 20742, USA*

† Electronic supplementary information (ESI) available. See DOI: https://doi.org/10.1039/d4sm01343c

‡ These authors contributed equally to this work.

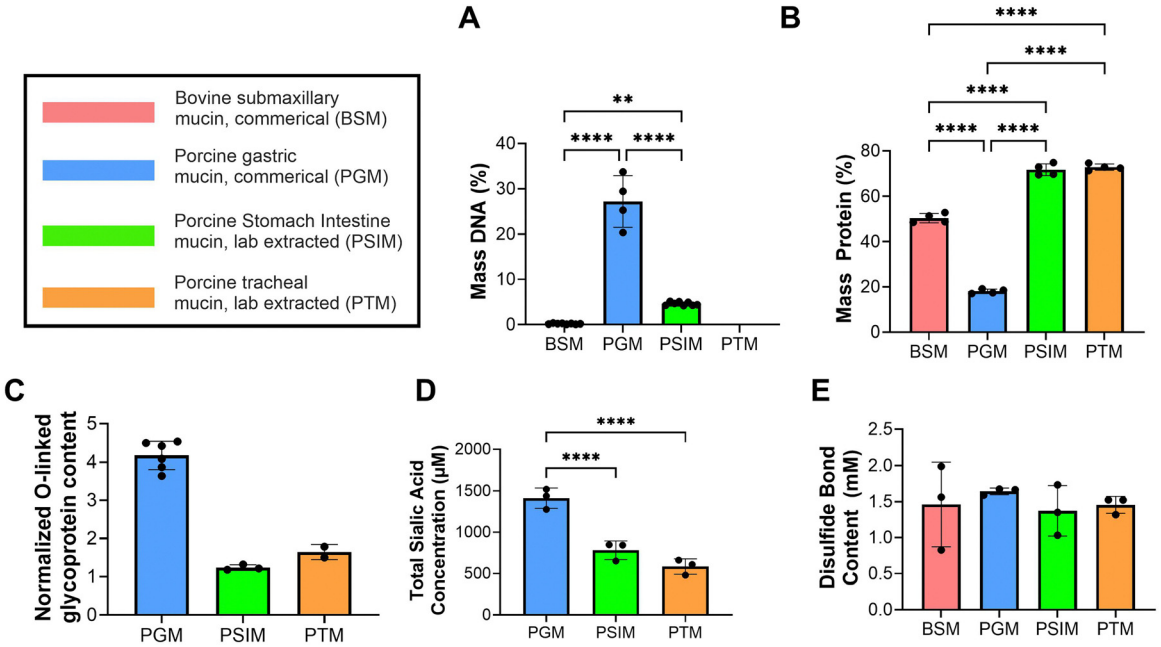


Fig. 1 Biochemical characterization of commercial and lab-extracted mucins. (A)–(E) Commercially available BSM, commercially available PGM, laboratory extracted PSIM, and laboratory extracted PTM were characterized to determine (A) % mass DNA content, (B) % mass protein, (C) *O*-linked glycoprotein (mucin) content normalized to the fluorescence intensity of 1 mg $mL^{-1}$ BSM, (D) sialic acid content, and (E) disulfide bond content. All measurements in (A)–(E) were carried out on samples with 2% w/v solid concentration. Bars indicate mean with error bars for standard deviations and individual measurements are shown as data points. Data sets statistically analyzed with ANOVA: $*p < 0.05$, $**p < 0.01$, and $****p < 0.0001$. Comparisons are not significant ($p > 0.05$) unless noted otherwise. Due to the limited sample size for PTM ($n = 2$) for *O*-linked glycoprotein assessment, no statistical analyses were performed for the data in part (C).

patient-derived *ex vivo* airway mucus, as it is not widely available, and *in vitro* tissue culture derived airway mucus is not easy to produce in large quantities.[19,24] Moreover, reconstituted mucins are advantageous to study the concentration-dependent behavior of mucus gels. Motivated by this, we used an extraction protocol, adapted from previous work,[25,26] to isolate mucins from the porcine trachea without the need for advanced protein separation and purification techniques. A description of the porcine trachea mucin isolation procedure is provided in the ESI.†

We first evaluated the composition of PTM using a series of biochemical assays (Fig. 1). For comparison, we conducted these analyses on commercial mucins (BSM and PGM) as well as PSIM extracted using the same protocol. The resulting measurements revealed that lab extracted mucins, PTM and PSIM, contained minimal DNA, comparable to BSM, and significantly lower DNA than PGM (Fig. 1A). Both lab-extracted mucins contained a protein mass of ~70%, which was significantly higher than both BSM and PGM (Fig. 1B). Furthermore, we used dynamic light scattering to confirm the presence of large macromolecules within our samples for PSIM ($D_h$ = 9.37 ± 3.0 μm), which was greater than commercially available PGM ($D_h$ = 1.22 ± 0.04 μm) (Fig. S1, ESI†). The measured sizes of PSIM solutions would be indicative of higher-order mucin oligomers, whereas PGM solutions likely contain mucins in a monomeric form.[27–29] Notably, PGM yielded high *O*-linked glycoprotein (mucin) content, whereas PTM and PSIM yielded similar *O*-linked glycoprotein content to BSM (Fig. 1C). We also quantified the content of terminal sialic acid glycans as these are relevant to many homeostatic and disease-associated processes in the airway. We found that the sialic acid concentrations were similar in PSIM and PTM (Fig. 1D). In comparison to PGM, the extracted mucins (PSIM and PTM) contained significantly less total (*i.e.*, both free and mucin-associated) sialic acid. Given that lab extracted mucins possess less sialic acid compared to commercially produced PGM, it is possible that our extraction method reduces free and/or mucin-associated sialic acid content. We also should note that the modified Warren assay which our sialic acid protocol employs has been reported to have difficulty fully hydrolyzing sialic acid groups on BSM.[30] As such, the sialic acid content for BSM was not included in our results. Disulfide bond content was comparable between all mucin types (Fig. 1E). Collectively, these data support that mucins from pig tracheal tissue can be successfully harvested with this procedure.

We then performed microrheological assessment of these mucins to evaluate their gel-forming capacity and usefulness as a model for studies on the biophysical properties of mucus gels. Specifically, we used multiple particle tracking of nanoparticle (NP) probes to evaluate the viscoelastic properties of PSIM and PTM prepared at a physiological solid concentration of 2% and 4% w/v. To mimic the ionic strength and pH commonly found in the lungs, mucins were reconstituted in a physiological buffer containing 154 mM NaCl, 3 mM $CaCl_2$, and 15 mM $NaH_2PO_4$ at pH 7.4. Based on representative trajectories and measured mean squared displacement, NP was highly mobile within PSIM, whereas NP diffusion appeared significantly constrained within PTM (Fig. 2A). Based on the slope of the MSD *versus* time lag, the

 

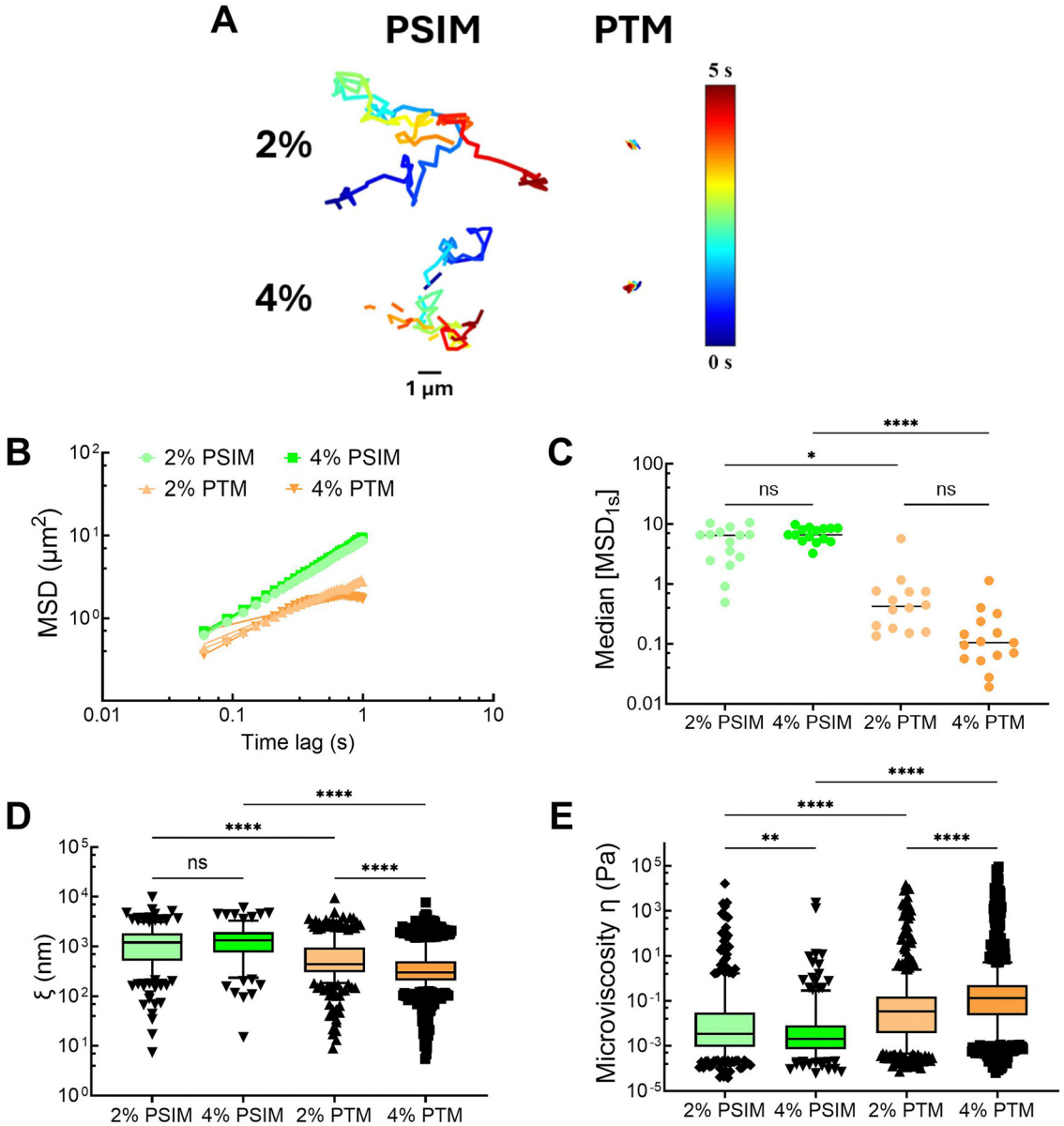


Fig. 2 Microrheology of porcine small intestine and tracheal mucins. (A) Representative trajectories of 100 nm (diameter) NP diffusion in 2% and 4% w/v of PSIM and PTM. Trajectory colors change as a function of time with 0 s indicated by dark blue and 5 s indicated by dark red. Scale bar = 1 μm. (B) Mean squared displacement *versus* time lag for NP diffusion in 2% and 4% w/v of PSIM and PTM. (C) Calculated median MSD at a time scale of 1 second ($MSD_{1s}$) for NP diffusion in 2% and 4% w/v of PSIM and PTM. Each data point represents the median calculated $MSD_{1s}$ in each video with 3–5 videos collected in 3 technical replicates. The bar in (C) indicates the average of measured median MSD values. Data set statistically analyzed with ANOVA: *$p < 0.05$, ****$p < 0.0001$, and ns = not significant. (D) Estimated pore size ($\xi$) and (E) microviscosity ($\eta$) at a frequency of 1 Hz from NP diffusion. (D) and (E) Each data point is an estimated pore size or microviscosity for each individual particle analyzed. Black lines indicate interquartile range. The data set was statistically analyzed with the Kruskal–Wallis test with Dunn's test for multiple comparison: ns = not significant, ****$p < 0.0001$, **$p < 0.01$.

anomalous diffusion exponent ($\alpha$) was determined by fitting the data from $\tau$ = 0.1–1 s. A value of $\alpha \approx 1$ is indicative of free (Brownian) nanoparticle diffusion in a purely viscous liquid whereas $\alpha$ should be less than 1 for subdiffusive movement for nanoparticles suspended in a gel network with viscoelastic properties.[31] NP exhibited Brownian diffusion in PSIM with $\alpha$ of 0.95 and 0.96 for 2% and 4% w/v concentrations, respectively. Conversely, subdiffusive NP motion was observed in PTM with $\alpha$ of 0.63 and 0.38 for 2% and 4% w/v PTM, respectively (Fig. 2B). We also find that the median MSD at $\tau$ = 1 s in 2% and 4% w/v PTM is significantly reduced as compared to PSIM (Fig. 2C). The mean pore sizes for PSIM were ~1.5–3 fold larger than in PTM where the average pore sizes were ~1.3–1.4 μm in PSIM and ~500–750 nm in PTM (Fig. 2D). The mean microviscosity for PSIM was higher at 2% than 4% w/v concentration. In comparison to PSIM, PTM possessed a ~1.5-fold greater microviscosity at 2% w/v and a ~20-fold greater microviscosity at 4% w/v PTM (Fig. 2E). Additional studies were also conducted comparing PTM and BSM, which showed that PTM possessed smaller pore sizes and greater microviscosity (Fig. S2, ESI†). Based upon

these data, PTM appeared to form a gel network whereas PSIM remained a solution at both 2 and 4% w/v concentrations. This may be due to the slightly higher *O*-glycosylation of PTM and/or differences in mucin composition as it is anticipated that PSIM is primarily MUC2 whereas PTM is a mixture of MUC5B and MUC5AC. Additional studies are needed to fully characterize how the chemical differences in MUC2 as compared to the airway mucins, MUC5B and MUC5AC, yield the observed differences in gel-forming capacity for PTM and PSIM and what influence pH has on their rheological properties.

To determine how the microrheological properties of PTM compared to a traditionally used airway mucus model, we collected airway mucus from differentiated human airway epithelial (HAE) tissue cultures. Prior studies by our group have shown that mucus collected from HAE cultures possess a total solid concentration ranging from 2–4% w/v.[32] Considering this, the microrheological properties of 2% and 4% w/v PTM were compared to HAE mucus. NP trajectories in HAE mucus were observed to be comparable to 2% PTM, whereas diffusion was much more restricted in 4% PTM (Fig. 3A). Given the qualitative similarities, we quantitatively compared the measured $MSD_{1s}$, pore size, and microviscosity for 2% PTM and HAE mucus. While similar in magnitude, we found a significant decrease in $MSD_{1s}$ and pore size, indicative of a tighter mesh network in 2% PTM (Fig. 3B and C). PTM also possessed a greater microviscosity compared to HAE mucus (Fig. 3D). These results could be explained by effective differences in mucin composition (*e.g.* molecular weight, relative amounts of MUC5B and MUC5AC) in PTM *versus* HAE mucus due to their distinct origins. Overall, these studies suggest that PTM can form into a gel with similar physical structure to tissue culture-derived airway mucus and may be suitable as a model to study airway mucin function.

Overall, this study establishes a method to create reconstituted airway mucin gels with physiologically relevant biophysical properties. For researchers interested in using PTM to model or study how airway mucus gel properties alter disease processes, we recommend using a 2% w/v PTM gel to simulate conditions in healthy airways whereas higher PTM concentrations (*i.e.* $\geq$4% w/v) would be appropriate conditions reflective of disease states such as asthma, chronic obstructive pulmonary disease (COPD), and cystic fibrosis (CF).[2] Beyond their relevance to airway disease research, this also provides a means to further evaluate the tissue-specific biophysical properties of mucus gels to establish important structure to function relationships. Given the notable differences in gel formation for PTM and PSIM at near neutral pH, we plan to perform further analysis of the pH-dependent assembly and rheological behavior of mucins derived from the lungs, intestines, and potentially other tissues in future studies.

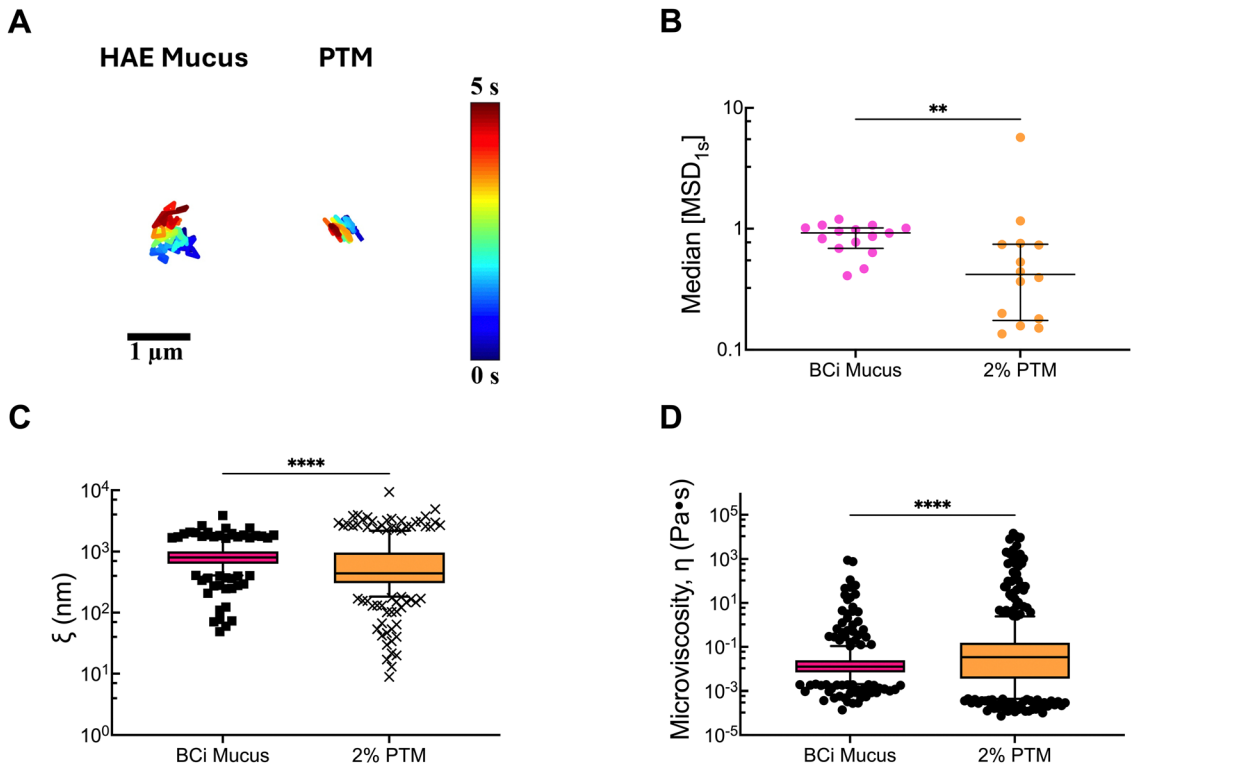


Fig. 3 Microrheology of human airway cell culture and porcine tracheal mucins. (A) Representative trajectories of 100 nm (diameter) NP diffusion in BCi mucus from HAE cultures and 2% w/v PTM. Trajectory colors change as a function of time with 0 s indicated by dark blue and 5 s indicated by dark red. Scale bar = 1 μm. (B) Calculated median MSD at a time scale of 1 second ($MSD_{1s}$) for NP diffusion in BCi mucus and 2% w/v of PSIM and PTM. Each data point represents the median calculated $MSD_{1s}$ in each video with 3–5 videos collected in 3 technical replicates. Black lines indicate interquartile range. (C) Estimated pore size ($\xi$) from NP diffusion. (D) Estimated microviscosity ($\eta$) from NP diffusion. (C) and (D) Each data point is an estimated pore size or microviscosity for each individual particle analyzed. Data was statistically analyzed with Kruskal–Wallis test with Dunn's test for multiple comparisons: ns = not significant, ****$p < 0.0001$, **$p < 0.01$.

 

## Data availability

The data supporting this article have been included as part of the ESI.†

## Conflicts of interest

The authors have no conflicts of interest to declare.

## Acknowledgements

This study was funded by the Cystic Fibrosis Foundation (DUNCAN24G0), the National Science Foundation (CBET 2129624), and the NIH (R21 EB030834, F31HL176146 awarded to A. B., R01 HL160540, HL160540-S1 awarded to S. Y.), and the University of Maryland (Grand Challenges Grant Program GC18).

## References

1 R. Bansil and B. S. Turner, Mucin structure, aggregation, physiological functions and biomedical applications, *Curr. Opin. Colloid Interface Sci.*, 2006, **11**(2–3), 164–170.
2 D. Song, D. Cahn and G. A. Duncan, Mucin Biopolymers and Their Barrier Function at Airway Surfaces, *Langmuir*, 2020, **36**(43), 12773–12783.
3 R. A. Cone, Barrier properties of mucus, *Adv. Drug Delivery Rev.*, 2009, **61**(2), 75–85.
4 S. K. Lai, Y. Y. Wang, D. Wirtz and J. Hanes, Micro- and macrorheology of mucus, *Adv. Drug Delivery Rev.*, 2009, **61**(2), 86–100.
5 D. J. Thornton, K. Rousseau and M. A. McGuckin, Structure and Function of the Polymeric Mucins in Airways Mucus, *Annu. Rev. Physiol.*, 2008, **70**(1), 459–486.
6 C. E. Wagner, K. M. Wheeler and K. Ribbeck, Mucins and Their Role in Shaping the Functions of Mucus Barriers, *Annu. Rev. Cell Dev. Biol.*, 2018, **34**, 189–215.
7 M. E. V. Johansson, H. Sjövall and G. C. Hansson, The gastrointestinal mucus system in health and disease, *Nat. Rev. Gastroenterol. Hepatol.*, 2013, **10**(6), 352–361.
8 M. E. V. Johansson, J. M. H. Larsson and G. C. Hansson, The two mucus layers of colon are organized by the MUC2 mucin, whereas the outer layer is a legislator of host–microbial interactions, *Proc. Natl. Acad. Sci. U. S. A.*, 2011, **108**(1), 4659–4665.
9 M. I. Pino-Argumedo, A. J. Fischer, B. M. Hilkin, N. D. Gansemer, P. D. Allen and E. A. Hoffman, *et al.*, Elastic mucus strands impair mucociliary clearance in cystic fibrosis pigs, *Proc. Natl. Acad. Sci. U. S. A.*, 2022, **119**(13), e2121731119.
10 L. S. Ostedgaard, T. O. Moninger, J. D. McMenimen, N. M. Sawin, C. P. Parker and I. M. Thornell, *et al.*, Gel-forming mucins form distinct morphologic structures in airways, *Proc. Natl. Acad. Sci. U. S. A.*, 2017, **114**(26), 6842–6847.
11 B. A. Symmes, A. L. Stefanski, C. M. Magin and C. M. Evans, Role of mucins in lung homeostasis: regulated expression and biosynthesis in health and disease, *Biochem. Soc. Trans.*, 2018, **46**(3), 707–719.
12 E. Iverson, L. Kaler, E. L. Agostino, D. Song, G. A. Duncan and M. A. Scull, Leveraging 3D Model Systems to Understand Viral Interactions with the Respiratory Mucosa, *Viruses*, 2020, **12**(12), 1425.
13 S. Tuve, H. Wang, J. D. Jacobs, R. C. Yumul, D. F. Smith and A. Lieber, Role of Cellular Heparan Sulfate Proteoglycans in Infection of Human Adenovirus Serotype 3 and 35, *PLoS Pathog.*, 2008, **4**(10), e1000189.
14 M. Cohen, X. Q. Zhang, H. P. Senaati, H. W. Chen, N. M. Varki and R. T. Schooley, *et al.*, Influenza A penetrates host mucus by cleaving sialic acids with neuraminidase, *Virol. J.*, 2013, **10**(1), 321.
15 G. Petrou and T. Crouzier, Mucins as multifunctional building blocks of biomaterials, *Biomater. Sci.*, 2018, **6**(9), 2282–2297.
16 M. Marczynski, K. Jiang, M. Blakeley, V. Srivastava, F. Vilaplana and T. Crouzier, *et al.*, Structural Alterations of Mucins Are Associated with Losses in Functionality, *Biomacromolecules*, 2021, **22**(4), 1600–1613.
17 G. A. Duncan, J. Jung, A. Joseph, A. L. Thaxton, N. E. West and M. P. Boyle, *et al.*, Microstructural alterations of sputum in cystic fibrosis lung disease, *JCI Insight*, 2016, **1**, 18.
18 L. Kaler, K. Joyner and G. A. Duncan, Machine learning-informed predictions of nanoparticle mobility and fate in the mucus barrier, *APL Bioeng.*, 2022, **6**(2), 026103.
19 M. R. Markovetz, D. B. Subramani, W. J. Kissner, C. B. Morrison, I. C. Garbarine and A. Ghio, *et al.*, Endotracheal tube mucus as a source of airway mucus for rheological study, *Am. J. Physiol.: Lung Cell. Mol. Physiol.*, 2019, **317**(4), L498–L509.
20 B. S. Schuster, J. S. Suk, G. F. Woodworth and J. Hanes, Nanoparticle diffusion in respiratory mucus from humans without lung disease, *Biomaterials*, 2013, **34**(13), 3439–3446.
21 L. R. Bonser, L. Zlock, W. Finkbeiner and D. J. Erle, Epithelial tethering of MUC5AC-rich mucus impairs mucociliary transport in asthma, *J. Clin. Invest.*, 2016, **126**(6), 2367–2371.
22 D. J. Thornton, T. Gray, P. Nettesheim, M. Howard, J. S. Koo and J. K. Sheehan, Characterization of mucins from cultured normal human tracheobronchial epithelial cells, *Am. J. Physiol.: Lung Cell. Mol. Physiol.*, 2000, **278**(6), L1118–L1128.
23 D. B. Hill, P. a Vasquez, J. Mellnik, S. a McKinley, A. Vose and F. Mu, *et al.*, A biophysical basis for mucus solids concentration as a candidate biomarker for airways disease, *PLoS One*, 2014, **9**(2), 1–11.
24 K. Joyner and G. A. Duncan, Reliably sourced airway mucus, *Am. J. Physiol.: Lung Cell. Mol. Physiol.*, 2019, **317**(4), L496–L497.
25 A. Sharma, J. G. Kwak, K. W. Kolewe, J. D. Schiffman, N. S. Forbes and J. Lee, *In Vitro* Reconstitution of an Intestinal Mucus Layer Shows That Cations and pH Control the Pore Structure That Regulates Its Permeability and Barrier Function, *ACS Appl. Bio. Mater.*, 2020, **3**(5), 2897–2909.
26 S. Yang and G. A. Duncan, Synthetic mucus biomaterials for antimicrobial peptide delivery, *J. Biomed. Mater. Res., Part A*, 2023, **111**(10), 1616–1626.
27 X. Cao, R. Bansil, K. R. Bhaskar, B. S. Turner, J. T. LaMont and N. Niu, *et al.*, pH-Dependent Conformational Change of

Gastric Mucin Leads to Sol-Gel Transition, *Biophys. J.*, 1999, **76**(3), 1250–1258.

28 A. Curnutt, K. Smith, E. Darrow and K. B. Walters, Chemical and Microstructural Characterization of pH and [$Ca^{2+}$] Dependent Sol-Gel Transitions in Mucin Biopolymer, *Sci. Rep.*, 2020, **10**(1), 8760.

29 D. J. Thornton and J. K. Sheehan, From mucins to mucus: toward a more coherent understanding of this essential barrier, *Proc. Am. Thorac. Soc.*, 2004, **1**(1), 54–61.

30 The Colorimetric Analysis of Sialic Acid in Human Saliva and Bovine Salivary Mucin, [cited 2024 Sep 18], Available from: **https://journals.sagepub.com/doi/epdf/10.1177/00220345780570111701**.

31 K. Joyner, S. Yang and G. A. Duncan, Microrheology for biomaterial design, *APL Bioeng.*, 2020, **4**(4), 041508.

32 D. Song, E. Iverson, L. Kaler, A. Boboltz, M. A. Scull and G. A. Duncan, MUC5B mobilizes and MUC5AC spatially aligns mucociliary transport on human airway epithelium, *Sci. Adv.*, 2022, **8**(47), eabq5049.

 